Surface Science 657 (2017) 1–9

Contents lists available at ScienceDirect

Surface Science

journal homepage: www.elsevier.com/locate/susc

The promotion of CO dissociation by molybdenum oxide overlayers on rhodium

Imre Szenti, László Bugyi*, Zoltán Kónya

MTA-SZTE Reaction Kinetics and Surface Chemistry Research Group, Department of Applied and Environmental Chemistry, University of Szeged, Rerrich Béla sqr. 1, 6720 Szeged, Hungary

A B S T R A C T

A considerable promotional effect of MoO_x species observed at high pressures on the catalytic activity of rhodium initiated the present UHV model study. The MoO_x overlayers formed on Rh films (0.15–20.0 ML) supported by TiO_2(110) substrate were characterized by AES, TPD, work function (WF) measurements and CO adsorption. On the mixed oxide support produced by depositing 1.2 ML Mo onto TiO_2(110), a new recombinative CO desorption state was observed with T_p=700 K, assigned as β-CO and related to the promotional effect of MoO_x species diffused onto Rh particles of 1.0 ML coverage. The development of β-CO needs 0.5–0.7 ML threshold Rh coverage, attributable to particle size effect and geometric factors governing the CO adsorption. The β-CO state with T_p=725–742 K could also be detected on Rh films covered by MoO_x moiety formed by the oxidation of Mo overlayers in O_2. Remarkably, recombinative CO desorption with T_p=700 K could be observed on the Rh nanoparticles covered by MoO_zC_y produced from pure Mo deposits by CO adsorption, too. In harmony with the promotional effect of MoO_x overlayer found at high pressures, it is established that the dissociation of CO is maximal at 0.2–0.3 ML Mo coverage, attributed to the presence of active sites at the oxide-metal interface. The low desorption peak temperature (700 K) of associative CO desorption observed in the presence of MoO_x and MoO_zC_y overlayers indicates a low activation energy for the reactions of O_a and C_a atoms, allowing high reaction rates for these intermediates. The MoO_x species exerted both promotion and inhibition effects on CO adsorption at sub-monolayer coverages, but above 1 ML it completely suppressed the reactivity of rhodium layers towards CO, suggesting that its surface concentration is a critical factor.

1. Introduction

The shortage of platinum metals capable of catalyzing several industrially important reactions induces great efforts in the scientific community to make their application more efficient and more economical. It was recognized long ago that the catalytic performance of important, but rather expensive rhodium metal can be influenced advantageously by different additives, including molybdenum and its oxides [1]. Metal oxides are mostly involved in heterogeneous catalysis inherently since they are widely used to support the finely dispersed, catalytically active metal particles. Moreover, it turned out that the so-called reducible oxide supports, like MoO_x [1], TiO_x [2,3], FeO_x [4], etc., from which oxide particles can migrate onto the surface of metal nanoclusters, can act as promotors. Iron oxide in the form of encapsulation layer was found to exert promotional effect on the CO oxidation over a Pt catalyst [4]. It has been established by high pressure investigations that the rate of an industrially important reaction, the hydrogenation of CO is maximal at intermediate TiO_x coverages [5]. In harmony with this, we verified in a UHV model study that the extent of CO dissociation is also maximal at the same coverage range [6]. Besides the promotion of CO hydrogenation on Rh catalysts by MoO_x [1], molybdenum oxides were found to facilitate other reactions on different metals as well. The catalytic activity of Pt/Al_2O_3 catalyst in propane oxidation reaction significantly increased in the presence of molybdenum and tungsten oxide additives, accompanied by excellent thermal stability of the modified catalyst [7]. Remarkably, a considerable catalytic promotional effect of different reducible oxides, like MoO_x, TiO_x and CeO_x has been reported for the rather inert Au(111) surface [8] in the water gas shift (WGS) reaction. MoO_2 supported Au and Cu particles showed also outstanding activity in the WGS reaction and it was suggested that the oxide support was directly involved in the WGS process [9]. MoO_x-promoted Au/SiO_2 catalysts were found to be more active in reverse water-gas shift reaction (RWGS) by an order of magnitude than the un-promoted ones [10].

Some UHV model studies on the catalytic effect of molybdenum additives have also been performed. It was reported that on the Pt(111)

* Corresponding author.
E-mail address: sir@chem.u-szeged.hu (L. Bugyi).

http://dx.doi.org/10.1016/j.susc.2016.11.002
Received 10 June 2016; Received in revised form 17 October 2016; Accepted 5 November 2016
Available online 11 November 2016

surface, oxidized Mo deposits blocked the Pt surface sites leaving essentially unchanged the adsorption behavior of CO on the uncovered part of platinum [11], but in a high-pressure study it was suggested that at the Rh-MoO_x interface CO can be bonded through its C atom to the Rh and via its O atom to MoO_x [12]. It seems obvious that the more reduced is the MoO_x species, corresponding to lowering in x, the higher is its activity towards carbon monoxide and oxygen. As an extremity, a Mo-covered Pt(110) single crystal can be much more reactive than the bare or MoO_x-covered one [13,14]. The effect of a pure Mo overlayer on the reactivity of the supporting metal can hardly be established, since molybdenum mostly interacts with the reaction mixture. The reaction of Mo with oxidative reactants can occur even if it is covered completely by monolayer thick platinum metals [15]. Hence, as a result of the high affinity of Mo towards oxygen and due to the low surface free energy of the forming MoO_x species, under oxidation conditions the end product of a bimetallic platinum metal-molybdenum system can be a platinum metal covered by MoO_x, irrespective of the deposition sequence of platinum metal and molybdenum. Depending on the oxidative or reductive nature of reaction mixture, the molybdenum can be present with variable oxidation states and may show complex redox properties. It has been reported that the oxidation state of Mo in an additive and the surface composition of Mo-Rh catalyst nanoparticles can be changed considerably in oxidative and reductive gases [16]. Consequently, it is desirable to carry out experiments with well-defined molybdenum oxides to elucidate the mechanism of their catalytic promotion. UHV model studies on MoO_x modified Rh catalysts can eliminate several variables being present in real catalysis, making possible to identify the important factors influencing the catalyst activity and stability.

The hydrogenation of carbon monoxide on Rh was found to be greatly promoted in the presence of molybdenum oxide [12], and the experimental data suggested a mechanism including enhanced CO dissociation. It has been reported that the Mo:Rh content must be 0.6 for the sake of optimal hydrogenation activity of amides [17]. For the promotion of WGS reaction on Pt, the Mo:Pt ratio had to be less than 0.7 [18], and a complete deactivation of Pt sites for CO hydrogenation was found at higher Mo load [12]. In harmony with these findings, in our previous model study we found that the reactivity of MoO_2 and MoO_3 supported Rh particles (0.4 ML) towards CO was completely suppressed after an annealing to 600 K due to MoO_x migration to the rhodium [19]. To adjust finely the surface concentration of MoO_x species, two methods are applied in the present work. First, self-assembled MoO_x overlayers are formed on Rh particles supported by mixed titanium molybdenum oxides by heat treatments. The redox reactions between molybdenum deposits and TiO_2(110) substrate, surveyed in details in the literature [20], provide reliable recipes for producing mixed metal oxides. Second, MoO_x is produced by the oxidation of Mo overlayers in O_2 gas. As outlined above, molybdenum additives on Rh are expected to exert a catalytic promotional effect on CO dissociation, however, in our previous study MoO_x originating form MoO_2 and MoO_3 supports was only found to inhibit the CO adsorption [19]. In the present work we extend the former investigations to a MoO_x-Rh system capable of promoting the decomposition of CO.

2. Experimental

The experiments were performed in an ultrahigh vacuum (UHV) chamber (base pressure $< 5\times10^{-8}$ Pa) equipped with facilities for Auger electron spectroscopy (AES), and temperature programmed desorption (TPD). AES measurements were performed with a Physical Electronics coaxial-gun single pass cylindrical mirror analyzer (CMA), while mass spectrometric and TPD data were collected by a Balzers QMS 200 quadrupole mass spectrometer. A smooth polynomial was subtracted from each TPD spectrum as a baseline correction, applied also by others [21] and care was taken to avoid the generation of any additional TPD feature by this procedure. AES was performed in the differential mode with 3 keV primary electron energy, 3 V modulation, and 1–2 μA beam current. AES data were evaluated either plotting the absolute peak-to-peak heights of main peaks (Mo: 186 eV, Rh: 302 eV, Ti: 387 eV, O: 503 eV, C: 272 eV) or Auger ratios calculated from these peaks. Work function (WF) was measured by two methods. First, it was determined by recording the cut-off energy of inelastic secondary electrons excited by the AES beam. The sample bias was −19 V and the relative WF values were derived by an accuracy of around 0.1 eV comparing the positions of the inflexion points in the current vs. voltage curves [22] with that for the nearly stoichiometric TiO_2(110) surface. Second, sensitive non-contact WF measurements were performed in a temperature-programmed manner [23] by a Besocke type Kelvin-probe with a sensitivity of 1 meV.

The TiO_2(110) single-crystal was the product of PI-KEM. The sample was attached to a Ta plate with an oxide glue (Aremco, Ceramabond 571), and could be heated with a W filament placed behind the Ta plate. The sample temperature was measured by a chromel–alumel thermocouple, attached to the side of the sample with the same adhesive material. To avoid the fracture of titania single crystal, the heating and cooling rates during cleaning and all measurements presented here were always less than 2 K/s, regulated by a computer-controlled circuit. The duration of annealing in stepwise heating experiments was equal to or less than 1 min.

The typical cleaning procedure of titania consisted of Ar^+-ion bombardment (1.5 keV, 1×10^{-7} A cm^{-2}, 300 K, 30 min) and annealing at 1000 K for 30 min. The absence of oxygen-treatments resulted in blue-colored, defective crystal. Note, that after this procedure the contribution of Ti^{3+} and Ti^{2+} signals to the Ti 2p photoemission feature was found to be below 3%, according to XPS measurements performed in another vacuum chamber. The above treatment ensured the appropriate electrical conductivity for electron spectroscopy and high enough defect-density to observe 2D-like growth of Rh-particles in extended coverage range, which allowed the estimation of surface coverage through AES measurements [24]. 1 monolayer (ML) Rh coverage corresponds to a Rh surface concentration, where, supposing a 2D film growth on a TiO_2(110) single-crystal, the Rh LEIS signal would disappear [25]. This method was verified by AES measurements, through following the growth of Rh layer on Mo multilayer which is known to obey a layer-by-layer growth mode [26], giving a well-defined break-point in the Mo AES signal intensity at 1 ML Rh coverage. It is known from previous STM investigations that the above sample treatment results basically in (1×1) bulk terminated registry, although the presence of 1–2% of defect sites (0D dots and 1D strings of Ti_2O_3 stoichiometry) cannot be excluded [27]. This surface is mentioned throughout this article as a nearly stoichiometric titania and is designated as s-TiO_2(110).

An EGN4 e-beam evaporator of Oxford Applied Research was used for the deposition of Rh and Mo by physical vapor deposition (PVD) at a sample temperature of 300–330 K. The oxidation of molybdenum layers (0.1–1.2 ML) was performed via reaction with the titania support, or by heating in 1×10^{-6} mbar O_2 for 20 min at 560 or 650 K.

3. Results and discussion

3.1. Properties of Rh particles supported by mixed molybdenum-titanium oxide

In our former study it was verified by LEIS measurements that the extent of thermally assisted encapsulation of 1.0 ML thick Rh film was somewhat modified by 1.2 ML Mo pre-deposited onto the TiO_2(110) substrate [28]. Since it has been found that the TiO_x species migrated to the Rh promotes the dissociation of adsorbed CO [2,6], to clarify the promotional effect of MoO_x overlayer, the extent of encapsulation of Rh by MoO_x and TiO_x species on the Mo pre-covered titania is to be estimated. For comparison with previous LEIS data [28], the effect of heating on the surface composition of a 1.0 ML thick Rh layer

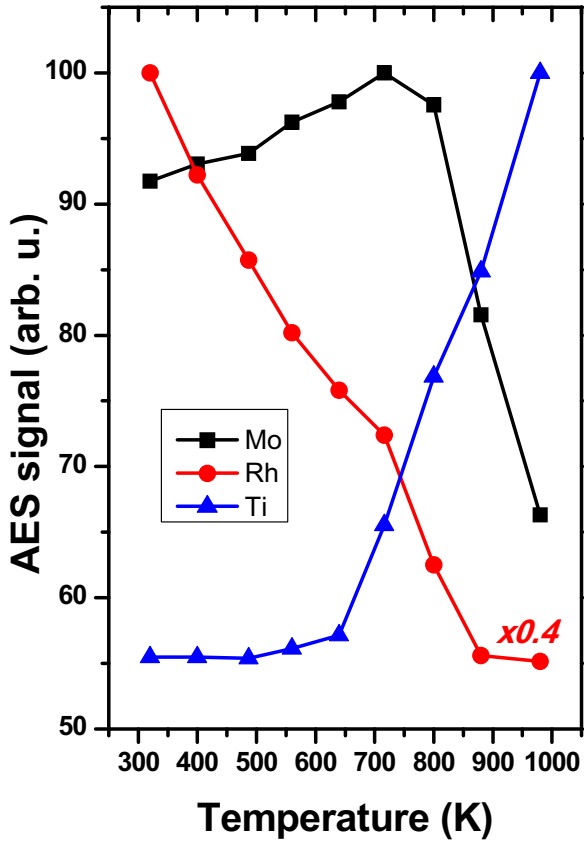

Fig. 1. Mo, Rh and Ti AES signal intensities as a function of temperature for a TiO_2(110) crystal covered by 1.2 ML Mo and 1.0 ML Rh.

deposited on the titania, pre-covered with 1.2 ML Mo was followed by AES, see ***Fig. 1.*** On annealing to 720 K, the Rh AES signal reduced by about 30%, and both the Mo and Ti signals enhanced, which can be explained by the encapsulation of Rh particles by MoO_x and TiO_x species, completing by about 700 K as proven by the disappearance of Rh LEIS signal shown in a previous study [28]. Although Rh clusters (0.4 ML) on a TiO_2(110) support do not aggregate up to 700 K [29], this cannot be completely ruled out for the particles supported by the Mo-covered titania, giving a possible contribution to the Mo AES signal enhancement (***Fig. 1***). Above 720 K, the decay in Rh AES peak intensity accompanied by the Ti signal enhancement can partly be due to the aggregation of Rh particles. The decrease in Mo AES signal above 720 K can be attributed to an extended oxidation of Mo-deposit to MoO_2 and MoO_3 through redox reaction with the substrate and above 800 K to the sublimation of MoO_3 to the gas phase [30]. It was found in an earlier study that above 500 K the outermost surface region loses Mo [28]. The decay in surface Mo concentration on annealing at 500–1000 K is accompanied by a 0.75 eV decrease in WF (not shown), which can also be correlated with the diffusion of Mo into the defect sites of titania lattice and with the sublimation of MoO_x species. Considering the lower WF of TiO_x overlayer [31], 0.6 eV, as compared with that of MoO_x [19], 1.0 eV, the WF decrease above 500 K can be related to the increase of TiO_x coverage on Rh particles at the expense of MoO_x species.

To reveal the details of the surface chemistry of Rh particles (1.0 ML) supported by the Mo covered (1.2 ML) titania, the effect of stepwise heating was followed by CO titration, as presented in ***Fig. 2A***. Note that CO does not desorb from the Rh-free, Mo-covered titania surface after 20.0 L of CO exposure. The molecular α-CO desorption characterized with T_p=460 and 570 K is suppressed after pre-annealing to 480 and 630 K, while a new state, designated as β-CO, showing broad feature at 700 K without pre-annealing, appears and is shifted to

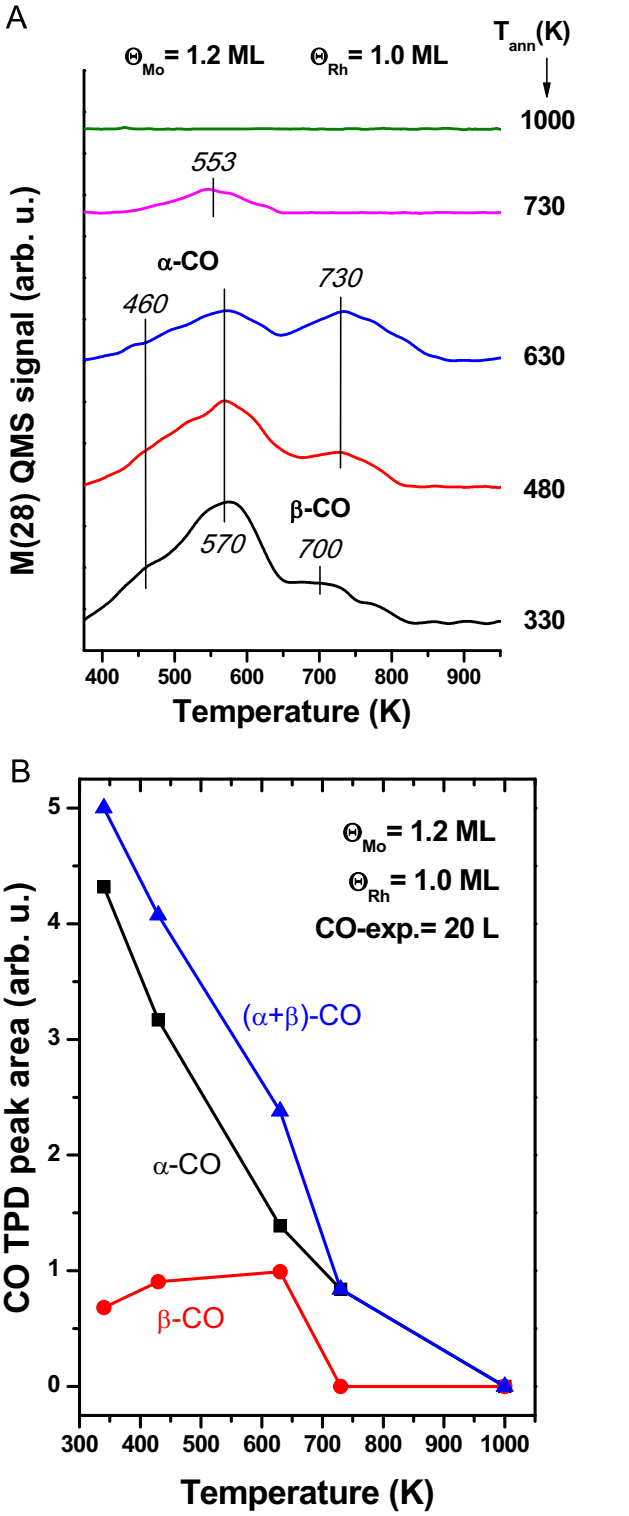

Fig. 2. (A) CO desorption from the s-TiO_2(110)+1.2 ML Mo+1.0 ML Rh surface pre-annealed to the indicated temperatures and exposed to 20.0 L of CO at 300 K. (B) Desorption peak areas for the molecular and recombinative CO states as a function of pre-annealing temperature. Lines serve as guide to the eyes.

730 K. The β-CO state developed with T_p=700 K can be associated with a recombinative CO desorption affected by the MoO_x surface species, which was found to migrate easily to the Rh particles from the MoO_2 and MoO_3 supports between 330 and 600 K [19]. After pre-annealing to 630 K, the β-CO peak became asymmetric and a shoulder appeared at around 770 K. A comparison with former findings reveals that the

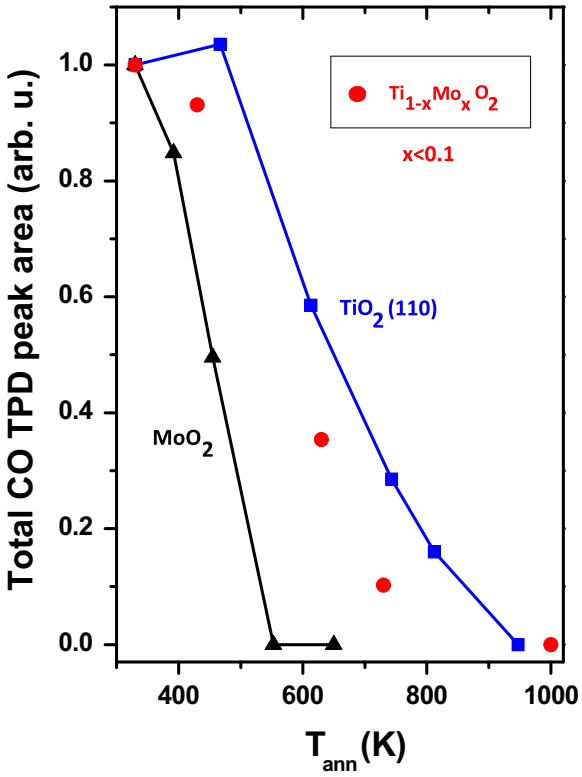

Fig. 3. Normalized total amounts of desorbed CO from the MoO_2, TiO_2 and $TiO_{1-x}Mo_xO_2$ surfaces covered by 0.4 ML Rh, pre-annealed to different temperatures and saturated with 20.0 L of CO at 300 K.

broadening of this feature may be the consequence of some TiO_x migration to the Rh particles, which is known to generate a recombinative γ-CO state with T_p=765 K [6]. After pre-annealing to 730 K, the desorption states above 650 K are completely eliminated. Further annealing to 1000 K removed all the CO desorption features, which is in agreement with a former observation regarding the inhibition effect of a continuous, pure TiO_x layer on CO adsorption [6]. The quantitative evaluation of CO desorption is presented in ***Fig. 2B***, where it is illustrated again that the β-CO state evolved already at 330 K, reflecting that MoO_x can migrate to the Rh particles at this temperature. In ***Fig. 3***, comparison of the normalized total amounts of desorbed CO (***Fig. 2***) with that from TiO_2 and MoO_2 supported Rh particles [19] reveals that on the Mo covered titania (designated as $Ti_{1-x}Mo_xO_2$, see the reasoning below) the amount of desorbed CO up to 720 K pre-annealing temperature is between those found for the pure oxides. For Rh nanoparticles supported by MoO_2 the CO desorption ceases after pre-annealing to 550 K due to the migration of a rather mobile and inactive MoO_x species onto the metal [19]. The above findings support that the species which cover the Rh supported by the mixed titanium molybdenum oxide have an apparent intermediate mobility between that of TiO_x and MoO_x. Up to 550 K mostly MoO_x may cover the surface and above 550 K the surface concentration of TiO_x can be enhanced.

The formation of mixed molybdenum-titanium oxide following the deposition of 1.2 ML Mo on the TiO_2(110) substrate can be inferred from literature findings. It is established that in the interfacial reaction of Mo and TiO_2(110) surface a maximum oxidation state of +4 can be reached in a molybdenum deposit at 300 K [30]. The similarity between the structure of rutile TiO_2 and monoclinic MoO_2 allows a limited mixing (5–6%) of these oxides, while at higher concentrations of MoO_2 phase separation occurs [21]. Following the decomposition of $Mo(CO)_6$ and a subsequent heat treatment at 853 K in air, the formation of a substitutional near-surface alloy with a stoichiometry of $Ti_{1-x}Mo_xO_2$ ($x < 0.1$) was found [32], corresponding to Mo^{4+} ions embedded in the titania lattice. Although the replacement of Ti^{4+} ions with Mo^{4+} ions needs thermal treatment [21,32], the WF changes of the Mo-covered TiO_2(110) sample [19] indicate that it occurs to some extent even at 420 K. Accordingly, the surface composition of support during stepwise heating (***Figs. 2*** and ***3***) can be assigned as $Ti_{1-x}Mo_xO_2$ with the remark that x is increasing during the heating process.

Taking into account the desorption peak temperatures for the recombinative CO states shown in ***Fig. 2A***, it is reasonable to suppose that from the $Ti_{1-x}Mo_xO_2$ mixed oxide below 500 K mostly MoO_x migrates to the Rh, but above this temperature the overlayer formed is composed of mixed MoO_x and TiO_x layer. It is remarkable that the promotional effect for CO dissociation on the mixed oxide support is maximized at lower pre-annealing temperature, 630 K (***Fig. 2***), as on the titania-supported Rh particles, 700 K [6]). This can be explained with the higher mobility of MoO_x species originating from the mixed molybdenum titanium oxide as compared with that of TiO_x stemming from TiO_2(110). Importantly, the recombinative CO desorption occurs with lower desorption peak temperature in the presence of MoO_x (700 K, ***Fig. 2***) than under the influence of TiO_x (765 K, [6]), meaning that in a catalytic reaction the removal of surface O and C atoms takes place with lower activation energy, allowing higher reaction rate.

To investigate the effect of temperature on the mobility of MoO_x species originating from the mixed molybdenum titanium oxide, on the Mo covered (1.2 ML) titania 1 ML thick Rh layer was also formed at 200 K (not shown). It is known from XPS data that the extent of redox reaction between titania and Mo at this low temperature is the same as at 300 K [28], hence the production of similar MoO_x species can be expected in both cases. A CO adsorption-desorption experiment revealed that on the layer produced at 200 K no recombinative β-CO state formed, verifying that at this temperature MoO_x species could not migrate onto the Rh particles.

It is to be considered that the dissociation of CO on titania supported Rh particles was found to occur only above a threshold Rh coverage, ~0.2 ML [24], what can be related with coverage dependent structural and electronic features characteristic of the metal deposit and with metal substrate interaction [33]. To reveal a possible particle size effect, the influence of Rh coverage on the decomposition of adsorbed CO was investigated on the Mo-covered titania support. In ***Fig. 4*** it can be seen that at 1.2 ML Mo pre-coverage two molecular CO states populate, with T_p~420 K and with T_p=493 K. The apparent upward shift in the peak temperature of the latter one above 0.5 ML Rh coverage can partly be due to overlapping with the broad β-CO feature appearing at around 700 K. The formation of β-CO state begins only at a threshold coverage range, Θ_{Rh}=0.5–0.7 ML. To explain this phenomenon it must be considered that the CO dissociation activity of Rh particles has been found to be correlated with the availability of highly coordinated adsorption sites which depends on the size and shape of nanoparticles [34]. For CO dissociation an ensemble of metal atoms in a particular geometry capable of binding the CO molecule and its dissociation products can be an important factor [35]. In other words, to bind the O and C adatoms, a minimum number of Rh atoms are needed in the Rh particles. It was found that the CO dissociation activity of alumina supported Rh particles depended on the island size, exhibiting a maximum for islands with around 1000 atoms [33], which was correlated with the presence of highly coordinated adsorption centers on Rh particles, the formation of which requires obviously a minimum number Rh atoms. In addition, it is important to emphasize, that the electronic band structure, determining the chemical reactivity of metal deposits, also depends on the number of constituent atoms of metal particles [33]. These effects can contribute to the appearance of the threshold Rh coverage observable in ***Fig. 4***, corresponding to an average Rh particle size below which the reactivity towards the CO molecule is suppressed even in the presence of a reactive MoO_x moiety.

The surface processes were also followed by temperature-programmed WF measurements performed with a Kelvin-probe, see the inset in ***Fig. 4***. This method which monitors around 7 square

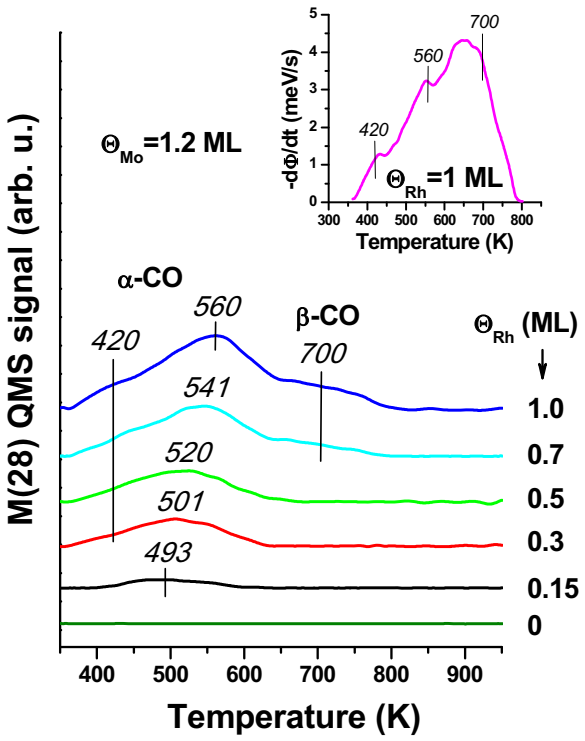

Fig. 4. CO TDS traces for different amounts of Rh deposited on the TiO_2(110) surface pre-covered by 1.2 ML Mo and exposed to 20.0 L of CO at 300 K. Inset: the negative derivative of the surface work function as a function of temperature, taken at the same heating rate and metal coverages as the uppermost TDS curve.

millimeter area in the middle of the sample, rules out the contribution of gas desorption from the back and edge of the sample to the WF signal, which, on the contrary, may exert some influence on the TPD spectra [36]. The molecular and recombinative CO desorption states could be detected by the Kelvin-probe also as overlapping features at 1.2 ML Mo pre-deposition and 1.0 ML Rh coverage. In comparison with the corresponding, uppermost TPD spectrum of ***Fig. 4***, the amount of molecular state seems less than that of recombinative one. This can be associated with the dipole moment of adsorbed states [23]. Accordingly, the dissociation products, O and C adatoms seems to have a larger average dipole moment than the CO molecule. Note that good coincidence was found in the shape and location of normalized TPD spectra and the negative derivative of temperature-dependent WF signals on the surfaces where molecular CO desorption prevailed, i.e. on Rh multilayers.

3.2. The effect of oxidized and pure Mo overlayers on the reactivity of Rh nanoparticles towards CO

To suppress the possible contribution of TiO_x overlayer on the surface chemistry of TiO_2(110) supported Rh nanoparticles, the effect of oxidized Mo overlayers on CO adsorption has also been addressed. In ***Fig. 5A*** it is demonstrated how the MoO_x species produced from its elements on the top of 1.0 ML thick Rh film influences the thermal desorption of CO. The Mo coverage varied between 0.1 and 0.5 ML, and the Mo deposits were oxidized in 10^{-6} mbar O_2 for 20 min at 650 K. A similar treatment of Mo multilayer resulted in the formation of molybdenum oxide with a high WF of 7.0 eV, attributed to MoO_3 [19] and it was established that under similar conditions the oxidation number of Mo deposited on titania raised above +4 [30]. Note that a control thermal desorption spectroscopy (TDS) experiment verified that from the mixed molybdenum titanium oxide no CO desorption occurred following 20.0 L gas exposure. In ***Fig. 5*** it can be seen that at 0.1 ML Mo coverage the MoO_x suppressed the α-CO states at T_p=440

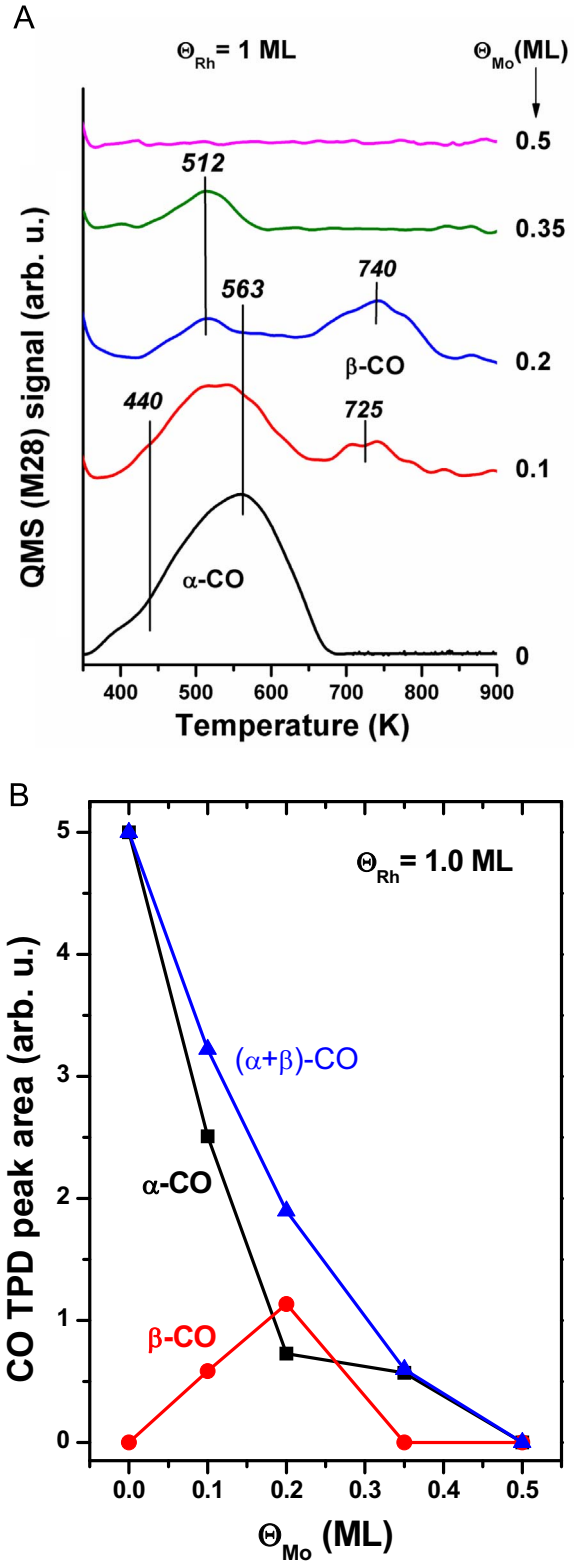

Fig. 5. (A) CO desorption from the MoO_x covered Rh particles (1.0 ML) after exposing the surface to 20.0 L of CO at 300 K. MoO_x was formed by the oxidation of the Mo deposits at 560 K in 10^{-6} mbar O_2 lasting for 20 min. (B) The corresponding integrated peak areas for the molecular and recombinative CO states as a function of Mo coverage. Lines serve as guide to the eyes.

and 563 K, but generated a new, broad CO desorption feature with T_p=725 K, which can be identified as the recombinative β-CO state. The state with T_p=563 K can be ascribed to molecular CO adsorbed at on-top, while the one with T_p=440 K at bridge position [24]. Repulsive

adsorbate-adsorbate interaction can contribute to the broadening of TDS traces. At Θ_{Mo}=0.2 ML the α-states are further reduced, the β-CO is intensified and its T_p is shifted to 740 K. At Θ_{Mo}=0.35 ML the β-CO is eliminated, but the α-CO with T_p=512 K is still present. The concerted suppression of α-CO states at T_p=563 K and T_p=440 K reflects the bonding of MoO_x species on the corresponding adsorption centers with similar probabilities, resulting in a narrow TDS feature with T_p=512 K at 0.35 ML Mo coverage. At Θ_{Mo}=0.50 ML all CO desorption ceased, revealing a complete hindrance of CO adsorption. Although the size and shape of titania supported Rh nanoparticles was found unaltered by STM up to 700 K during the encapsulation with TiO_x species [29], structural changes of Rh particles covered by MoO_x cannot be ruled out on annealing. The determination of change in the particle size from CO desorption experiments is not straightforward, since different CO adsorption states develop which require different number of surface sites on Rh (***Fig. 5A***). However, it can be estimated that the size of Rh clusters is not changing substantially in the presence of MoO_x overlayer and adsorbed CO, since the total amount of desorbed CO as a function of MoO_x coverage decreases approximately linearly (Fig. 5***B***).

Clearly, in ***Fig. 5*** the amount of dissociative β-CO state goes through maximum with the increase of the MoO_x coverage, hence the formation of this state can be associated with the overall number of perimeter sites. The disappearance of the β-CO at Θ_{Mo}=0.35 ML can be due to the coalescence of MoO_x species into larger islands resulting in a strong reduction in the number of active MoO_x perimeter sites. If the coalesced islands are large enough, the concentration of β-CO drops below the detection limit of TDS, but a fraction of the surface may still remain free to allow molecular CO adsorption. Note that in ***Fig. 2A*** the appearance of α-CO following a thermal treatment at 730 K can be explained similarly, that is with the aggregation of MoO_x and TiO_x species, leaving enough adsorption centers for molecular CO bonding. It is important to note that the position of α-CO desorption peaks varies only slightly with the MoO_x coverage in ***Fig. 5A***, which is indicative of a weak interaction between MoO_x overlayer and rhodium, allowing a simple site-blocking effect. This mechanism was also observed for a MoO_x covered Pt(110) single crystal as deduced from CO adsorption experiments [14]. On the other hand, the appearance of recombinative β-CO state reflects the presence of reactive MoO_x species on Rh. Similarly, in a high pressure study [8] reactive CeO_x, TiO_x and MoO_x moieties were found to generate water dissociation even on the rather indifferent Au(111) single crystal.

To exclude any pre-annealing of the Mo-covered rhodium clusters before TPD experiments, the titania supported Rh films were covered by different amounts of Mo metal and their reactivity was tested through CO adsorption (20.0 L). In ***Fig. 6A*** it is demonstrated that enhancing the coverage of metallic Mo from 0.2 ML to 1.0 ML on a 1.0 ML thick Rh film strongly suppresses the amount of α-CO state with T_p=570 K, but leaves nearly intact the other state with T_p~450 K. The γ-CO with T_p=885 K on the Mo-free titania originates from the titania-rhodium interface [24], and is eliminated at and above 0.2 ML Mo coverage. Noticeably, the β-CO with T_p=700 K also appears on the Mo-covered Rh particles, and it is detectable even at Θ_{Mo}=2.0 ML. Its amount has a maximum at Θ_{Mo}=0.5 ML (***Fig. 6B***), suggesting that the recombination of C and O atoms proceeds at the molybdenum-rhodium interface. Considering the unvaried and low, 700 K peak temperature for the associative CO desorption at 0.2–2.0 ML Mo coverages, it is reasonable to suppose that it originates not from the inner part of Mo islands, where the O and C atoms are more highly coordinated to Mo atoms, but from their perimeter sites where weaker binding occurs. If the O and C atom containing, 2.0 ML thick Mo layer forms 3D structures, the MoO_zC_y-Rh interface represents adsorption sites where the recombinative CO state can still be populated. Molecular CO desorption at this coverage may be absent if the 3D structures are produced only during the heating cycle of TPD experiment.

The question arises whether the CO dissociation could be observed on Mo-covered platinum metals in previous model studies. It has been

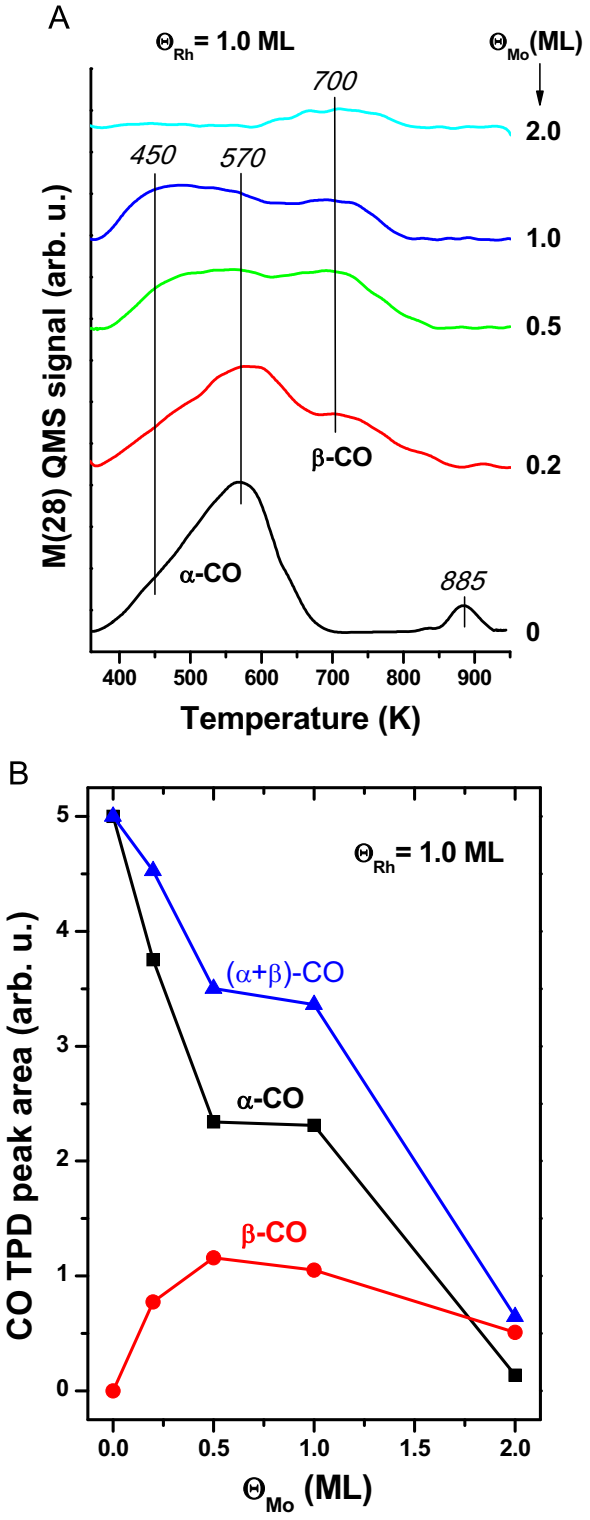

Fig. 6. (A) CO desorption from Rh particles (1.0 ML) covered by different amounts of Mo, after exposing the surface to 20.0 L of CO at 300 K. (B) Integrated peak areas for the molecular α-CO and dissociative β-CO states. Lines serve as guide to the eyes.

established that the oxidation state of molybdenum in a deposit can greatly influence the reactivity of a platinum metal [13]. As an extremity, a Pt(110) single crystal covered by metallic molybdenum is more reactive than the bare or MoO_x-covered one [14]. After exposing a Pt(110) crystal to 10.0 L $Mo(CO)_6$ at 100 K a CO TDS feature appearing at 540 K was associated with CO desorption from the Mo deposit [13]. In addition, CO desorption was detected with T_p=575

and 600 K after saturating the Pt(110) and Pt(110)+MoO_x surfaces with $Mo(CO)_6$. Since the latter peak temperatures are by more than 100 K higher than the T_p-s of molecular CO desorption for either Pt [13] or Mo [37] surfaces, the corresponding desorption states can be attributed to the recombination of C and O adatoms. Furthermore, AES proved that the surface C and O contaminants originating from the high temperature (700 K) decomposition of $Mo(CO)_6$ on the same Pt(110) surface could be completely eliminated by annealing to 1000 K [14]. These observations indicate that on a Mo-covered Pt(110) surface C and O atoms recombine above 500 K and below 1000 K, that is in the same temperature region, where associative CO desorption was found from the CO-saturated Rh+Mo and Rh+MoO_x surfaces. Accordingly, on different platinum metals the surface species produced by the oxidation of molybdenum deposits with the oxygen of dissociated CO, seems to have the potential to act as promotor in those catalytic reactions where the decomposition of CO is an intermediate step.

It is worth comparing the TDS data for CO desorption from MoO_x and Mo covered Rh surfaces, displayed in ***Fig. 5*** and ***Fig. 6***. First, it is to be considered that the MoO_x particles are reactive with CO only at their perimeter [11], [12], while the whole surface of Mo islands covering the Rh can react with CO. As a result, the inactive MoO_x layer [14] can completely suppress the reactivity of Rh towards CO adsorption at 0.5 ML Mo coverage that is the MoO_x species prepared can fully block the surface. On the contrary, the 2.0 ML thick Mo layer reacting with CO seems to be able to produce 3D structures, providing active reaction centers at the rhodium-molybdenum interface. It is remarkable that the temperature range for recombinative CO desorption is 800–1200 K on a macroscopic molybdenum surface [37], but from the perimeter of the nanosized, Rh supported Mo particles CO desorbs with T_p=700 K. This low temperature can be explained by the influence of the underlying rhodium and by the lowered coordination of surface Mo, C and O atoms to each other as compared with that in a 3D structure. Taking into account that on the Mo layer supported by Rh particles the CO adsorption results in O and C-atoms, on the one hand it is straightforward that the oxidation number of Mo cannot be 0 following CO exposures. On the other hand, the oxidation number of Mo must be lower than that reached by extensive oxidation in O_2 gas. Accordingly, Mo with oxidation number less than +6 is responsible for the promotional effect of MoO_zC_y particles on CO dissociation.

3.3. *The impact of MoO_x* species on the surface chemistry of CO on Ar^+-ion sputtered Rh multilayers

To eliminate completely the effect of TiO_2(110) support on the surface chemistry of Rh, MoO_x species was produced on Rh multilayers. To get rid of the trace amount of carbon being present in Rh multilayers after metal deposition, they were annealed to 1000 K to encapsulate them by TiO_x, which oxidized the carbon contamination. The TiO_x overlayer was removed by mild Ar^+-ion sputtering [6] and the clean Rh was covered by Mo and oxidized in O_2 stream at 560 K.

In ***Fig. 7*** the effect of annealing on the 20.0 ML thick Rh multilayer covered by MoO_x is displayed, as followed by AES and WF measurements. The points at 300 K correspond to a 1.0 ML thick Mo deposit. The oxidation performed at 560 K caused a small change in the Mo/Rh AES ratio, but was accompanied by a significant WF enhancement of 1.3 eV. The stepwise heating between 560 and 1000 K resulted in the gradual decrease of both the Mo/Rh AES ratio and WF. Remarkably, the former quantity indicated a nearly complete loss of Mo in the near-surface region after annealing at 1000 K. This is in harmony with the evaporation of volatile MoO_3 species above 800 K [30]. The elimination of MoO_x from the surface is accompanied by 1.1 eV WF decrease. A similar value, 1.0 eV was calculated for MoO_x species covering completely a 0.4 ML thick, MoO_3-supported Rh layer after annealing to 550 K [19], suggesting that the two species are similar. The high initial WF difference presented in ***Fig. 7***, 2.0 eV, related to the WF of nearly stoichiometric titania involves a high absolute WF of around 7.0 eV,

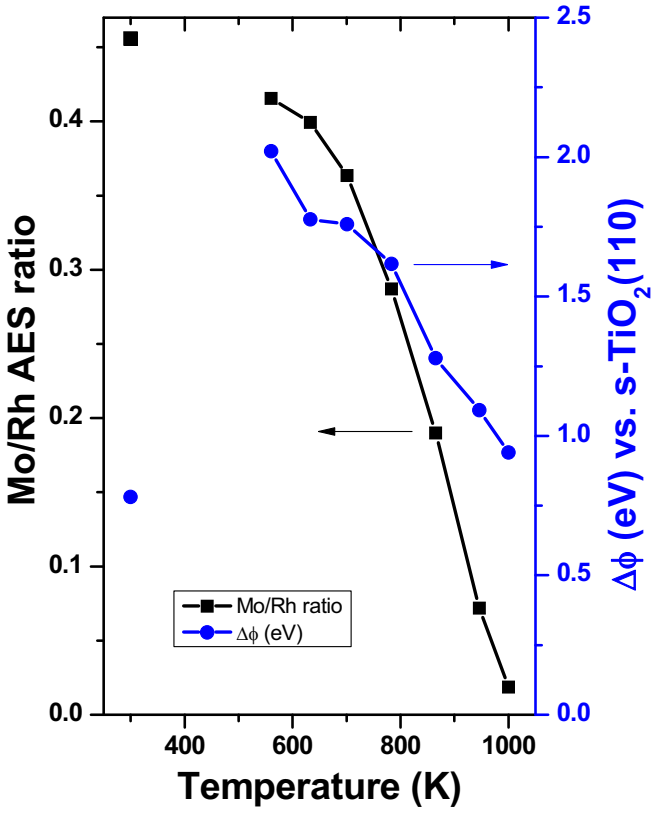

Fig. 7. The effect of annealing on the Mo/Rh AES ratio and work function of MoO_x covered, 20 ML thick Rh multilayer. The Mo coverage was 1.0 ML, and the oxidation process consisted of 20 min annealing in 10^{-6} mbar O_2 at 560 K. The points at 300 K belong to the Mo-covered Rh prior to oxidation.

which is close to that of bulk MoO_3 [19]. High dipole moments were also found for atomically thin MoO_x layers formed on graphene [38]. The question arises, how the thickness of a MoO_x overlayer correlates with its WF. Well-defined MoO_3 films could be prepared on the Au(111) surface with monolayer [39] and bilayer thickness [40]. It was established that the charge transfer between a molybdenum trioxide monolayer and the supporting metal can result in the reduction of molybdenum ions, corresponding to lower WF of the MoO_3 overlayer as compared with that of bulk oxide [41]. The WF was found to depend on the MoO_x layer thickness, being higher at higher oxide coverages. Since our MoO_x overlayer is characterized, as shown in ***Fig. 7***, by a WF of near to 7.0 eV, a value close to that of bulk MoO_3, it is probably composed of a bilayer.

In ***Fig. 8*** CO desorption signals are presented for MoO_x covered Rh multilayers saturated with CO at 300 K. It is demonstrated that increasing the coverage of MoO_x species, the T_p of the associative CO desorption (γ-CO, 812 K), characteristic of the ion-sputtered Rh film [6], decreases gradually, manifesting in the appearance of a broad TPD feature with T_p=785 K at Θ_{Mo}=0.2 ML. At higher molybdenum coverages, Θ_{Mo}=0.5 ML and Θ_{Mo}=0.75 ML the recombinative CO desorption is characterized by peaks at T_p=742 K. Overlapping molecular CO desorption states show TDS features peaked at 588 and 540 K, which are suppressed with the enhancement of MoO_x concentration. The development of β-CO with T_p=742 K can be attributed to the same process that was observed for Rh particles covered by MoO_x produced from 0.1–0.2 ML Mo (***Fig. 5***), namely to the MoO_x assisted dissociation of CO. The enhanced peak temperature for the recombinative CO desorption, 742 K, as compared with 725 K observed for Rh particles (***Fig. 5A***) can be due to the presence of defect sites generated by Ar^+-ion sputtering. Noticeably, the recombinative CO-desorption from a pure Mo multilayer (not shown) provides a much higher desorption

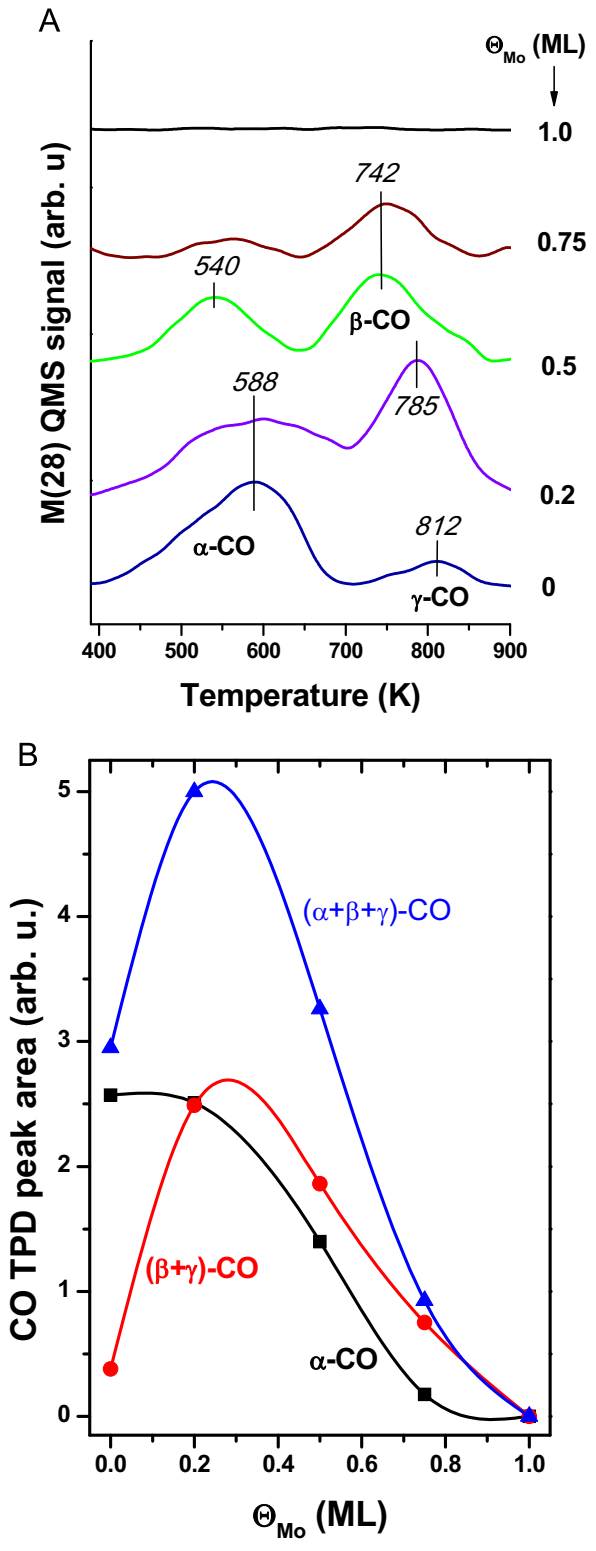

Fig. 8. (A) CO desorption traces for Ar^+-ion sputtered, 20 ML thick Rh multilayers covered by different amounts of MoO_x and saturated with 20.0 L of CO at 300 K. MoO_x was prepared by the oxidation of Mo deposits in 10^{-6} mbar O_2 at 560 K lasting for 20 min. (B) Molecular, recombinative and total CO desorption peak areas as a function of Mo coverage.

peak temperature, 950 K. Considering that in the presence of a 0.5 ML thick oxidized Mo overlayer the TDS peak characteristic of associative CO desorption is located at 742 K, that is at much lower temperature than on rhodium, 812 K, and on a molybdenum single crystal, 950 and 1050 K [37], it can be established that on a defect-rich Rh surface the MoO_x species promotes the decomposition of carbon monoxide. The extent of promotion is maximal at intermediate, 0.2–0.3 ML Mo coverage as shown in ***Fig. 8B***, similar to that presented in ***Fig. 5B*** for Rh nanoparticles, suggesting that the active sites for CO dissociation are located at the Rh-MoO_x interface on both surfaces.

As illustrated in ***Fig. 8***, for a Rh multilayer covered by MoO_x produced from 1.0 ML Mo and exposed to 20.0 L CO, any CO desorption is completely missing. Regarding the blocking effect of MoO_x species on CO adsorption, this observation is in harmony with our former finding [19] and with those for the Pt(111) [11] and Pt(110) [14] single crystals, supporting that a continuous MoO_x overlayer suppresses the reactivity of platinum metals towards carbon monoxide. Noticeably, the 0.75–1.0 ML Mo coverage range (***Fig. 8***), where the CO adsorption is completely suppressed on the ion-sputtered Rh film, is about twice as much as that for the Rh nanoparticles (***Fig. 5***). This can be explained by the preferential growth of 3D MoO_x particles in the atomic scale valleys of the ion-sputtered surface, which makes possible a hindered aggregation of MoO_x particles at 0.75 ML Mo coverage and the formation of β-CO at their perimeter sites.

The question arises what might be the oxidation number of molybdenum in the MoO_x species being active in CO dissociation. The characterization of ultrathin MoO_x layers has been addressed by XPS on several substrates. On graphene, Mo^{5+} and Mo^{6+} ions were detected for a 0.15 nm thick MoO_3 layer, but Mo^{6+} ions prevailed at 15 nm film thickness [38], suggesting a thickness effect. The activity of Au/SiO_2 catalysts in RWGS reaction increased by an order of magnitude as a result of promotion by MoO_x, in which Mo was found to be in +6 oxidation state [10]. MoO_2 supported Au and Cu particles showed outstanding activity in the WGS reaction and it was suggested that the oxide support, containing Mo^{4+} ions was directly involved in the WGS process [9]. A monolayer thick MoO_x species was found to be reducible by extended heat treatment on Au(111) [39], resulting in a stable composition containing 50% Mo^{5+} and 50% Mo^{6+} through the formation of extended 1D shear defects. According to the above findings and to a former suggestion that the CO molecule binds to the Rh supported oxide islands through a reduced metal center [12], it is reasonable to suppose that to exert a promotional effect, oxygen vacancies at the perimeter of oxide particles are needed where Mo ions with oxidation number less than the maximal +6 for Mo are present.

The present UHV study confirms the suggestion of former high pressure work regarding the promotion of CO dissociation by MoO_x species on Rh particles [12]. Clearly, the MoO_x overlayer is capable to generate recombinative β-CO state both on Rh nanoparticles and argon-ion sputtered Rh films. It has been proven that to observe the promotional influence of MoO_x overlayers on CO dissociation the Rh coverage must exceed a threshold coverage of 0.5–0.7 ML. Accordingly, at the 0.4 ML Rh coverage applied in our previous work [19] the promotion of CO decomposition was not observed. In harmony with the finding of high pressure studies that to promote maximally the hydrogenation reaction of CO [3], [5], the reducible oxide nanoparticles must be present on the Rh nanoparticles at intermediate submonolayer coverages, it is established that the optimal MoO_x concentration for CO decomposition corresponds to 0.2–0.3 ML Mo coverage (***Figs. 5B*** and ***8B***), supporting that the active centers are located at the Rh-MoO_x interface. The lowered peak temperature of recombinative CO desorption for the MoO_x modified rhodium nanoparticles, 700 K, as compared with that for the TiO_x-covered ones, 765 K [6], includes that the C and O atoms generated by CO dissociation are bonded less strongly to the surface in the presence of MoO_x species. During the catalytic hydrogenation of CO, at the perimeter of promotor oxide species the metal ions must pass through oxidation-reduction cycles [12]. The reduction of oxide overlayer proceeding through a reaction with adsorbed C atoms has lower activation energy if the CO desorption peak temperature is lower, predicting an easier reduction with hydrogen adatoms as well. According to the well-known volcano curve confirmed for many heterogeneous catalytic reactions, for optimal

catalytic activity the reaction intermediates must bind to the catalyst not too strongly and not too weakly [42], which seems to be valid for the C and O atoms on the MoO_x promoted rhodium surfaces, allowing high reaction rates in their further reactions.

Due to its low surface free energy and high surface mobility, the MoO_x species wets rhodium well, and for this reason on MoO_2 and MoO_3 supported Rh particles the CO adsorption was found to be completely blocked by the MoO_x overlayer at relatively moderate temperature, 600 K [19]. In the present study, the elimination of CO adsorption by MoO_x species was also observed at Θ_{Mo}=0.5 ML on Rh nanoparticles and Θ_{Mo}=1.0 ML on the Ar^+- ion sputtered Rh multilayers, respectively, pointing again to the necessity of low enough Mo/Rh mass ratio in a catalyst to avoid a complete inhibition effect.

4. Conclusions

i) Diffusion of MoO_x and TiO_x species from a Mo-covered (1 ML) titania to supported Rh particles (1 ML) at 330–1000 K was confirmed by AES and CO titration experiments.
ii) The MoO_x overlayer on a 1 ML thick Rh film generated a new recombinative CO desorption state with T_p=700 K, assigned as β-CO.
iii) On a Mo pre-covered (1.2 ML) TiO_2(110) surface the development of β-CO needs 0.5–0.7 ML threshold Rh coverage, attributable to Rh particle size effect and geometric factors governing the CO adsorption.
iv) The β-CO state can also be formed on 1.0 and 20.0 ML thick Rh films covered by MoO_x species prepared by the oxidation of Mo overlayers in O_2 and on Rh nanoparticles covered by MoO_zC_y species produced from pure Mo deposits by CO adsorption.
v) The amount of β-CO was maximized at 0.2–0.3 ML Mo coverage, supporting that it formed at the MoO_x–Rh interface, and that this sate is associated with the enhanced reactivity for CO hydrogenation found in high pressure studies. MoO_x hindered the molecular CO adsorption, underlining that the amount of this additive must be low for catalytic promotion.
vi) The low peak temperature (700 K) for the associative CO desorption on the MoO_x and MoO_zC_y modified Rh particles corresponds to a low activation energy in the recombination reaction of O_a and C_a atoms, which allows high reaction rates for these intermediates.

Acknowledgement

Supports through grants of the Hungarian Scientific Research Fund (OTKA) K120115, GINOP-2.3.2-15-2016-00013 and COST Action CM1104 are gratefully acknowledged.

References

[1] E.E. Lowenthal, L.F. Allard, M. Te, H.C. Foley, J. Mol. Catal. A-Chem. 100 (1995) 129.
[2] D.N. Belton, Y.-M. Sun, J.M. White, J. Catal. 102 (1986) 338–347.
[3] A. Boffa, C. Lin, A.T. Bell, G.A. Somorjai, J. Catal. 149 (1994) 149.
[4] M. Lewandowski, Y.N. Sun, Z.-H. Qin, S. Shaikhutdinov, H.-J. Freund, Appl. Catal. A: Gen. 391 (2011) 407–410.
[5] K. Hayek, M. Fuchs, B. Klötzer, W. Reichl, G. Rupprechter, Top. Catal. 13 (2000) 55.
[6] L. Bugyi, I. Szenti, Z. Kónya, Appl. Surf. Sci. 313 (2014) 432.
[7] Y. Men, G. Kolb, R. Zapf, H. Pennemann, V. Hesse, Chem. Eng. Res. Des. 87 (2009) 91–96.
[8] J.A. Rodriguez, S. Ma, P. Liu, J. Hrbek, J. Evans, M. Pérez, Science 318 (2007) 1757.
[9] J.A. Rodrıguez, P. Liu, J. Hrbek, M. Perez, J. Evans, J. Mol. Catal. A: Chem. 281 (2008) 59–65.
[10] R. Carrasquillo-Flores, I. Ro, M.D. Kumbhalkar, S. Burt, C.A. Carrero, A.C. Alba-Rubio, J.T. Miller, I. Hermans, G.W. Huber, George, J.A. Dumesic, J. Am. Chem. Soc. 137 (2015) 10317–10325.
[11] A.M. Robinson, M.M. Montemore, S.A. Tenney, P. Sutter, J.W. Medlin, J. Phys. Chem. C 117 (2013) 26716.
[12] B.J. Kip, E.G.F. Hermans, J.H.M.C. Van Wolput, N.M.A. Hermans, J. Van Grondelle, R. Prins, Appl. Catal. 35 (1987) 109–139.
[13] Z. Jiang, L. Xu, W. Huang, J. Mol. Catal. A: Chem. 304 (2009) 16–21.
[14] Z. Jiang, W. Huang, H. Zhao, Z. Zhang, D. Tan, X. Bao, J. Mol. Catal. A: Chem. 268 (2007) 213–220.
[15] W. Tang, G. Henkelman, J. Phys. Chem. C 130 (2009) 194504.
[16] D.A. Storm, F.P. Mertens, M.C. Cataldo, E.C. Decanio, J. Catal. 141 (1993) 478–485.
[17] G. Beamson, A.J. Papworth, C. Philipps, A.M. Smith, R. Whyman, J. Catal. 269 (2010) 93–102.
[18] W.D. Williams, L. Bollmann, J.T. Miller, W.N. Delgassa, F.H. Ribeiro, Appl. Catal. B: Environ. 125 (2012) 206.
[19] I. Szenti, L. Bugyi, Z. Kónya, Surf. Sci. 641 (2015) 60–67.
[20] Q. Fu, T. Wagner, Surf. Sci. Rep. 62 (2007) 431–498.
[21] O. Karshoglu, X. Song, H. Kuhlenbeck, H.-J. Freund, Top. Catal. 56 (2013) 1389–1403.
[22] L.J. Whitman, W. Ho, J. Chem. Phys. 89 (1981) 7621.
[23] T. Livneh, Y. Lilach, M. Asscher, J. Chem. Phys. 111 (1999) 11138.
[24] L. Bugyi, R. Németh, Surf. Sci. 605 (2011) 808.
[25] L. Óvári, L. Bugyi, Z. Majzik, A. Berkó, J. Kiss, J. Phys. Chem. C 112 (2008) 18011–18016.
[26] L.Q. Jiang, M. Strongin, Phys. Rev. B 42 (1990) 3292.
[27] A. Berkó, A. Magony, J. Szökő, Langmuir 21 (2005) 4562.
[28] L. Bugyi, L. Óvári, J. Kiss, Surf. Sci. 603 (2009) 2958–2963.
[29] A. Berkó, G. Ménesi, F. Solymosi, Surf. Sci. 372 (1997) 202.
[30] V. Blondeau-Patissier, B. Domenichini, A. Steinbrunn, S. Bourgeois, Appl. Surf. Sci. 175–176 (2001) 674–677.
[31] L. Bugyi, L. Óvári, Z. Kónya, Appl. Surf. Sci. 280 (2013) 60–66.
[32] G.A. Rizzi, A.E. Reeder, S. Agnoli, G. Granozzi, Surf. Sci. 600 (2006) 3345..
[33] M. Baumer, H.-J. Freund, Prog. Surf. Sci. 61 (1999) 127–198.
[34] S. Andersson, M. Frank, A. Sandell, A. Giertz, B. Brena, P.A. Bruhwiler, N. Martensson, J. Libuda, M. Baumer, H.-J. Freund, J. Chem. Phys. 108 (1998) 2967.
[35] M. Che, C.O. Bennett, Adv. Catal. 20 (1989) 153.
[36] J.M. Heitzinger, S.C. Gebhard, B.E. Koel, Surf. Sci. 275 (1992) 209–222.
[37] S. Raaen, X. Yu, Appl. Surf. Sci. 349 (2015) 17–20.
[38] J. Meyer, P.R. Kidambi, B.C. Bayer, C. Weijtens, A. Kuhn, A. Centeno, A. Pesquera, A. Zurutuza, J. Robertson, S. Hofmann, Sci. Rep. 4 (2014) 1.
[39] X. Deng, S.Y. Quek, M.M. Biener, J. Biener, D.H. Kanga, R. Schalek, E. Kaxiras, C.M. Friend, Surf. Sci. 602 (2008) 1166–1174.
[40] S. Guimond, D. Gobke, J.M. Sturm, Y. Romanyshyn, H. Kuhlenbeck, M. Cavalleri, H.-J. Freund, J. Phys. Chem. C 117 (2013) 8746.
[41] M.T. Greiner, L. Chai, M.G. Helander, W.-M. Tang, Z.-H. Lu, Adv. Funct. Mater. 23 (2013) 215–226.
[42] J.K. Norskov, T. Bligaard, J. Rossmeisl, C.H. Christensen, Nat. Chem. 1 (2009) 37.